Title

Systemic Retinaldehyde Treatment Corrects Retinal Oxidative Stress, Rod Dysfunction, and Impaired Visual Performance in Diabetic MiceSystemic Retinaldehyde Treatment in Diabetic Mice

Journal

Investigative Ophthalmology & Visual Science, 56(11)

ISSN

0146-0404

Authors

Berkowitz, Bruce A
Kern, Timothy S
Bissig, David
et al.

Publication Date

2015-10-02

DOI

10.1167/iovs.15-16990

Peer reviewed

Systemic Retinaldehyde Treatment Corrects Retinal Oxidative Stress, Rod Dysfunction, and Impaired Visual Performance in Diabetic Mice

Bruce A. Berkowitz,[1,2] Timothy S. Kern,[3] David Bissig,[1] Priya Patel,[1] Ankit Bhatia,[1] Vladimir J. Kefalov,[4] and Robin Roberts[1]

[1]Department of Anatomy and Cell Biology, Wayne State University School of Medicine, Detroit, Michigan, United States
[2]Department of Ophthalmology, Wayne State University School of Medicine, Detroit, Michigan, United States
[3]Department of Medicine, School of Medicine, Case Western Reserve University, Cleveland, Ohio, United States
[4]Department of Ophthalmology and Visual Sciences, Washington University School of Medicine, St. Louis, Missouri, United States

Correspondence: Bruce A. Berkowitz, Department of Anatomy and Cell Biology, Wayne State University School of Medicine, 540 East Canfield Street, Detroit, Michigan 48201, USA;
baberko@med.wayne.edu.

Submitted: March 30, 2015
Accepted: August 4, 2015

Citation: Berkowitz BA, Kern TS, Bissig D, et al. Systemic retinaldehyde treatment corrects retinal oxidative stress, rod dysfunction, and impaired visual performance in diabetic mice. *Invest Ophthalmol Vis Sci*. 2015;56:6294–6303. DOI:10.1167/iovs.15-16990

Purpose. Diabetes appears to induce a visual cycle defect because rod dysfunction is correctable with systemic treatment of the visual cycle chromophore 11-*cis*-retinaldehyde. However, later studies have found no evidence for visual cycle impairment. Here, we further examined whether photoreceptor dysfunction is corrected with 11-*cis*-retinaldehyde. Because antioxidants correct photoreceptor dysfunction in diabetes, the hypothesis that exogenous visual chromophores have antioxidant activity in the retina of diabetic mice in vivo was tested.

Methods. Rod function in 2-month-old diabetic mice was evaluated using transretinal electrophysiology in excised retinas and apparent diffusion coefficient (ADC) MRI to measure light-evoked expansion of subretinal space (SRS) in vivo. Optokinetic tracking was used to evaluate cone-based visual performance. Retinal production of superoxide free radicals, generated mostly in rod cells, was biochemically measured with lucigenin. Diabetic mice were systemically treated with a single injection of either 11-*cis*-retinaldehyde, 9-*cis*-retinaldehyde (a chromophore surrogate), or all-*trans*-retinaldehyde (the photoisomerization product of 11-*cis*-retinaldehyde).

Results. Consistent with previous reports, diabetes significantly reduced (1) dark-adapted rod photo responses (transretinal recording) by ~18%, (2) rod-dominated light-stimulated SRS expansion (ADC MRI) by ~21%, and (3) cone-dominated contrast sensitivity (using optokinetic tracking [OKT]) by ~30%. Both 11-*cis*-retinaldehyde and 9-*cis*-retinaldehyde largely corrected these metrics of photoreceptor dysfunction. Higher-than-normal retinal superoxide production in diabetes by ~55% was also significantly corrected following treatment with 11-*cis*-retinaldehyde, 9-*cis*-retinaldehyde, or all-*trans*-retinaldehyde.

Conclusions. Collectively, data suggest that retinaldehydes improve photoreceptor dysfunction in diabetic mice, independent of the visual cycle, via an antioxidant mechanism.

Keywords: ADC MRI, diabetes, MEMRI, oxidative stress, retina, transretinal recordings

Diabetic retinopathy is monitored and managed based on detection of retinal microangiopathy. The pathogenesis of diabetic microvascular histopathology involves retinal oxidative stress.[1,2] Recent evidence points to dysfunctional rod photoreceptor cells as a primary source of this oxidative stress.[1,3–6] Although the nature of the rod dysfunction is not entirely understood, it likely involves dysregulation of photoreceptor ion channels.[5,7–11] For example, rod cell calcium channels, which are normally open in the dark, are paradoxically closed in dark adapted diabetic mice as measured by manganese-enhanced MRI (MEMRI), the imaging modality of choice for studying retinal L-type calcium channel regulation in vivo.[3,12–22] In an initial study, diabetic mice treated with a single intraperitoneal (i.p.) injection of 11-*cis*-retinaldehyde, which is normally produced by the visual cycle, caused the paradoxically closed calcium channels in rod cells to partially open (3). These data, together with evidence from the published reports, suggest the hypothesis that diabetes impairs the visual cycle activity.[14,23–27] However, subsequent studies have not found any evidence for a visual cycle defect in diabetic mice.[28] Thus, the mechanism by which 11-*cis*-retinaldehyde exerts its beneficial action in the diabetic mouse retina is still unclear.

In diabetic mice, classical antioxidant approaches that prevent vascular histopathology also prevent the earlier abnormal ionic regulation in the retina, including in the rods as measured by MEMRI and apparent diffusion coefficient magnetic resonance imaging (ADC MRI).[5,11,29–31] Thus, we wondered if, as previously suggested by data in ex vivo assays,[32–35] retinaldehydes might be acting as antioxidants in diabetic mouse retina. If so, this could explain the beneficial impact of systemic retinaldehydes on improving dysfunctional rods in diabetes in vivo.[5,11,29–31]

The present study had three goals: (1) to confirm the correction of photoreceptor dysfunction using alternative (i.e., non-MEMRI) methods with 11-*cis*-retinaldehyde in diabetic mice; (2) to test for beneficial effects of 11-*cis*-retinaldehyde or 9-*cis*-retinaldehyde (a chromophore surrogate) on impaired cone-based visual performance of diabetic mice as measured by photopic optokinetic tracking (OKT) (Kirwin SJ, et al. *IOVS* 2010;51:ARVO E-Abstract 115; Barber AJ, et al. *IOVS* 2010;51:ARVO E-Abstract 109; Aung MH, et al. *IOVS* 2011;52:ARVO E-Abstract 5960)[36–40]; and (3) to test the hypothesis that exogenous retinaldehydes correct retinal oxidative stress in diabetic mice.

Methods

This study was performed in strict accordance with the National Institutes of Health Guide for the Care and Use of Laboratory Animals, the Association for Research in Vision and Ophthalmology Statement for the Use of Animals in Ophthalmic and Vision Research, and with authorization of the Institutional Animal and Care Use Committee at Wayne State University. Animals were housed and maintained in normal, 12L:12D light-dark cycle laboratory lighting, unless otherwise noted. All efforts were made to minimize suffering within the context of the diabetic protocol at all other times, including sub-therapeutic insulin to maintain weight and hydration treatment as needed (see details below).

Experimental Groups

At 2 months of age, 20-g male C57Bl/6 mice (Jackson Laboratories, Bar Harbor, ME, USA) were randomly divided into the following groups and were studied after 2 months of diabetes (or age-matched): (1) a non-diabetic control group (wild type [wt]); (2) a diabetic group (D); (3) a D+11-*cis*-retinaldehyde group (D+11-*cis*); and (4) a D+9-*cis*-retinaldehyde (D+9-*cis*); note that the ADC MRI data for groups i and ii were previously published (29). Retinaldehydes were delivered systemically. A subset of age-matched non-diabetic controls and diabetic mice were studied by electrophysiological examination (see below). In addition, in the following groups, rod-dominated retinal superoxide production was evaluated (see below): (1) a non-D control group (untreated and vehicle treated), (2) a D group; (3) a D+11-*cis*-retinaldehyde group(D+11-*cis*); (4) a D+9-*cis*-retinaldehyde (D+9-*cis*) group; and (5) a D+all-*trans*-retinaldehyde (D+all-*trans*) group.

In all cases, diabetes was similarly induced and maintained in mice. Mice with a starting weight of 16 to 20 g were injected with streptozotocin (60 mg/kg; 10 mM citrate buffer [pH 4.5]) i.p., within 10 minutes of preparation, once a day for 5 consecutive days. Body weight and blood glucose levels were monitored twice weekly. Insulin (neutral protamine Hagedorn; Humulin N; Eli Lilly, Indianapolis, IN, USA), was administered to mice as needed based on body weight and blood glucose levels but not more than twice weekly; mice were allowed slow weight gain while maintaining hyperglycemia (blood glucose levels higher than 400 mg/dL). Mice that lost weight and/or had blood glucose levels greater than 600 mg/dL were given 0.1 to 0.2 units of insulin. Normal rodent chow (11.2% fat, 26% protein, and 62.7% carbohydrate; Purina Test Diet 5001; Richmond, IN, USA) and water were provided ad libitum. Glycated hemoglobin (A1c) was measured from blood collected after each experiment.[6,29] Blood was drawn from the left ventricle, after puncture, into a capillary tube and stored in an Eppendorf tube with a small amount of heparin to prevent coagulation. The blood was kept at 4°C until analysis within 1 week following the experiment.

Treatments

11-*cis*-Retinaldehyde. Overnight dark-adapted diabetic mice were acutely treated with 11-*cis*-retinaldehyde (approximately 25 mg/kg mouse), obtained through NEI (https://www.nei.nih.gov/funding/11_*cis*_retinal.asp). The 11-*cis*-retinaldehyde was constituted in a 10% ethanol and phosphate buffered saline and BSA solution and administered as a 0.01 mL/g bolus intraperitoneal under dim red light 30 min before ADC MRI, OKT, and oxidative stress exams (see below).[23]

9-*cis*-Retinaldehyde. 9-*cis*-Retinaldehyde is effective with sustained delivery according to the study by Tang et al.[41] Under dim red light, 20 mg/kg 9-*cis* retinaldehyde (Toronto Research Chemicals, ON, Canada) was dissolved in 20 μL of 100% ethanol and combined with 180 μL of Matrigel (vehicle; catalog number 356234, BD Bioscience, MA, USA) at 4°C, as previously described.[41] In some mouse groups, vehicle with or without retinaldehyde was injected subcutaneously into the dorsal torso region several days prior to examination. Mice were then exposed to cyclic light for 2 days before being transferred to a dark room for 4 days per mouse.[41] OKT or oxidative stress measurements were performed (strict 30-min examination per mouse, see below for details) on the fourth day.

All-*trans* Retinaldehyde. All-*trans* retinaldehyde (Toronto Research Chemicals) was prepared, administered, and evaluated using the 9-*cis*-retinaldehyde procedure above.

OKT Examination. Two visual performance metrics were evaluated in awake and freely moving mice: spatial frequency thresholds (SFT; "acuity," in cycles/degree [c/d]) and contrast sensitivity (CS; measured at the peak of the nominal curve [0.064 c/d], inverse Michelson contrast [unitless]) using the optokinetic tracking reflex (unitless; OptoMotry; Cerebral Mechanics Inc., Alberta, Canada).[42] Briefly, a vertical sine wave grating was projected as a virtual cylinder in three-dimensional coordinate space on computer monitors arranged in a quadrangle around a testing arena. Unrestrained mice (after an overnight dark adaptation) were placed on an elevated platform at the center of the arena. An experimenter used a video image of the arena from above to view the animal and follow the position of its head with the aid of a computer mouse and a crosshair superimposed on the frame. The X-Y positional coordinates of the crosshair centered the hub of the virtual cylinder, enabling its wall to be maintained at a constant "distance" from the animal's eyes and thereby to fix the spatial frequency (SF) of the stimulus at the animal's viewing position. When the cylinder was rotated in a clockwise or counter clockwise direction, and the animal followed with head and neck movements that tracked the rotation, it was judged that the animal's visual system could distinguish the grating. Clockwise and counter-clockwise tracking provides a measure of left and right eye SFT and CS.[42] One set of SFT and CS measurements can reliably be obtained in 30 minutes.

Superoxide Production

In separate groups of mice, superoxide levels were measured chemically with lucigenin (bis-*N*-methylacridinium nitrate), as reported previously.[43–47] Each arm consisted of control, diabetic, and treated diabetic group evaluated on the same day.

Investigative Ophthalmology & Visual Science

Transretinal Recordings

On the day of the experiment, dark-adapted mice were killed by CO_2 asphyxiation, the retina was removed from the eyecup under infrared illumination, and a piece of it was mounted on filter paper with the photoreceptor side up on the recording chamber with an electrode connected to the bottom of the perfusion chamber. A second electrode was placed just above the center of the retina piece. The sample was perfused with Locke's solution containing 112.5 mM NaCl, 3.6 mM KCl, 2.4 mM $MgCl_2$, 1.2 mM $CaCl_2$, 10 mM HEPES, pH 7.2, 20 mM $NaHCO_3$, 3mM Na succinate, 0.5 mM Na glutamate, 0.02 mM EDTA, and 10 mM glucose. In addition, the solution was supplemented with 4 mM DL-aspartate and 10 mM DL-AP-4 to block higher-order components of the photoresponse[48] and with minimum essential vitamins and minimum essential amino acid solutions (Sigma-Aldrich Corp., St. Louis, MO, USA) to improve retina viability. The perfusion solution was continuously bubbled with a 95% O_2/5% CO_2 mixture and heated to 36–37°C. The electrode solution (140 mM NaCl, 3.6 mM KCl, 2.4 mM $MgCl_2$, 1.2 mM $CaCl_2$, 3 mM HEPES, 10 mM glucose, pH 7.4) in the lower electrode also contained 4 mM DL-aspartate and, in addition, 10 mM $BaCl_2$ to suppress the glial component of the photoresponse.[49]

Light stimulation was applied using 20-ms test flashes from a calibrated 505-nm light-emitting diode. Photo responses were amplified by a differential amplifier (DP-311; Warner Instruments, Hamden, CT, USA), low-pass filtered at 30 Hz (8-pole Bessel), digitized at 1 kHz, and stored in a computer file for further analysis. Half-saturating light intensity ($I_{1/2}$) was calculated from the intensity-response relationship as the test flash intensity required to produce a response with an amplitude equal to half of the corresponding saturated response amplitude. Data were analyzed using Clampfit version 10.2 (Molecular Devices, LLC, Sunnyvale CA, USA) and Origin 8.1 software (OriginLab Corp., Northampton, MA, USA).

MRI Procedures

The general mouse preparation for high resolution MRI is well established in our laboratory.[29] Briefly, all animals were maintained in darkness for at least 16 hours before and during the dark phase of MRI examination. High-resolution anatomical and ADC data were acquired on a 7-T system (ClinScan; Bruker, Ewing Twp., NJ, USA), using a receive-only surface coil (1.0-cm diameter) centered on the left eye. The end of a fiber optic bundle was attached to a light source (Mark II Light Source; Prescott, Inc., Monument, CO, USA) placed caudal to the eye, projecting at a white screen ~1 cm from the eye, similar to that previously described.[53] We exposed the eye to 0 (i.e., dark) or ~500 lux (confirmed outside the magnet by using a traceable dual-range light meter (Control Company, Friendswood, TX, USA) placed against a 1-cm-diameter aperture; measured this way, room lighting is ~300 lux). Aside from the fiber optic light source, all lights in the MRI room were turned off. In all groups, immediately before the MRI experiment, animals were anesthetized with urethane (36% solution intraperitoneally; 0.083 mL/20 g animal weight, prepared fresh daily; Sigma-Aldrich Corp.) and treated topically with 1% atropine to ensure dilation of the pupil during light exposure followed by 2% lidocaine to minimize responses that could lead to artifact-inducing eye motion. Anatomical and ADC (parallel to the optic nerve, the most sensitive direction for detecting changes at the location of the SRS[50]) MRI data sets were collected, first in the dark and then again 15 minutes after turning on the light. Because each ADC data set takes 10 minutes to collect, we refer to the mid-point in the ADC collection as 20 minutes of light exposure. Anatomical images were acquired using a spin-echo sequence (slice thickness of 600 μm, TR 1000 ms, TE 11 ms, matrix size 192 × 320, field of view 8 × 8 mm^2, NA 2). ADC data were collected using a modified diffusion-weighted spin-echo sequence (TR 1000 ms; slice thickness of 600 μm; TE, 33 ms; matrix size, 174 × 288; field of view, 8 × 8 mm^2; $b = 0$, 100, 250, 500, 600, 750, or 990 s/mm^2 collected in pseudo-random order; NA 1 per b value.[53] Images were registered and analyzed (using in-house code) to generate ADC profiles from the central retina as previously described.[53]

Raw MEMRI data do not allow ready visualization of cells within layers, as is possible with optical coherence tomography. Instead, layer locations are inferred based on the retinas well-defined laminar structure, clear anatomical landmarks like the vitreous-retina border, and highly localized functional changes within the retina. Thus, at the present resolution, we previously demonstrated that MRI can distinguish rod inner segment from outer segment based on the light-evoked expansion of the subretinal space in mice and rats, as well as, for example, (1) inner from outer retina manganese uptake as a function of light, (2) DIL-induced suppression of only inner retinal manganese uptake, and (3) the outer nuclear layer-only tetrameric visual arrestin 1 and its reduction via light-evoked translocation.[28,29,50,51] These examples strongly support our claim that the resolution of MRI is sufficient for extracting meaningful layer-specific functional data in vivo. In all cases, animals were humanely euthanized as detailed in our IACUC-approved protocol.

Data Analysis

In each animal that underwent MRI examination, we confirmed that the eyelid positions were sufficiently open based the anatomical MRI data; if eyelid position was such that it impeded the light path, only the dark data from that animal was used.[52] All eight images for each animal per lighting condition were registered (rigid body). We have previously demonstrated that a simplified estimate of ADC, as the slope describing progressive losses in (log-transformed) signal intensity at progressively higher diffusion weightings (b-values), is sufficient for observing dark / light changes in the SRS layer.[52] Thus, in this study, we calculated ADC as previously described.[52] In all cases, the same central retinal regions of interest (± 0.4–1 mm from the optic nerve head) were analyzed; thickness and ADC values from the superior and inferior retina were respectively averaged. ADC profiles in dark and light in each mouse were spatially normalized to retinal thickness values in the dark, as justified elsewhere.[29]

Statistical Analysis

Transretinal, OKT, and superoxide production data were consistent with those of a normal distribution and were compared using one-way ANOVA with post hoc 2-tailed t-test analyses. Due to insufficiently opened eyelids, we could not always collect both dark and light data from all animals. Also, the dark baseline ADC data was averaged from all wt groups regardless of subsequent light exposure. Comparison of ADC profile data between groups was performed using unpaired t-tests at different locations of the intra-retinal profiles. In addition, a generalized estimating equation (GEE) approach was also used to compare selected location ranges, identified from the t-tests as significant.[16,53] The GEE method performs a general linear regression analysis using contiguous locations in each subject and accounts for the within-subject correlation between contiguous locations. In all cases, $P \leq 0.05$ was

Investigative Ophthalmology & Visual Science

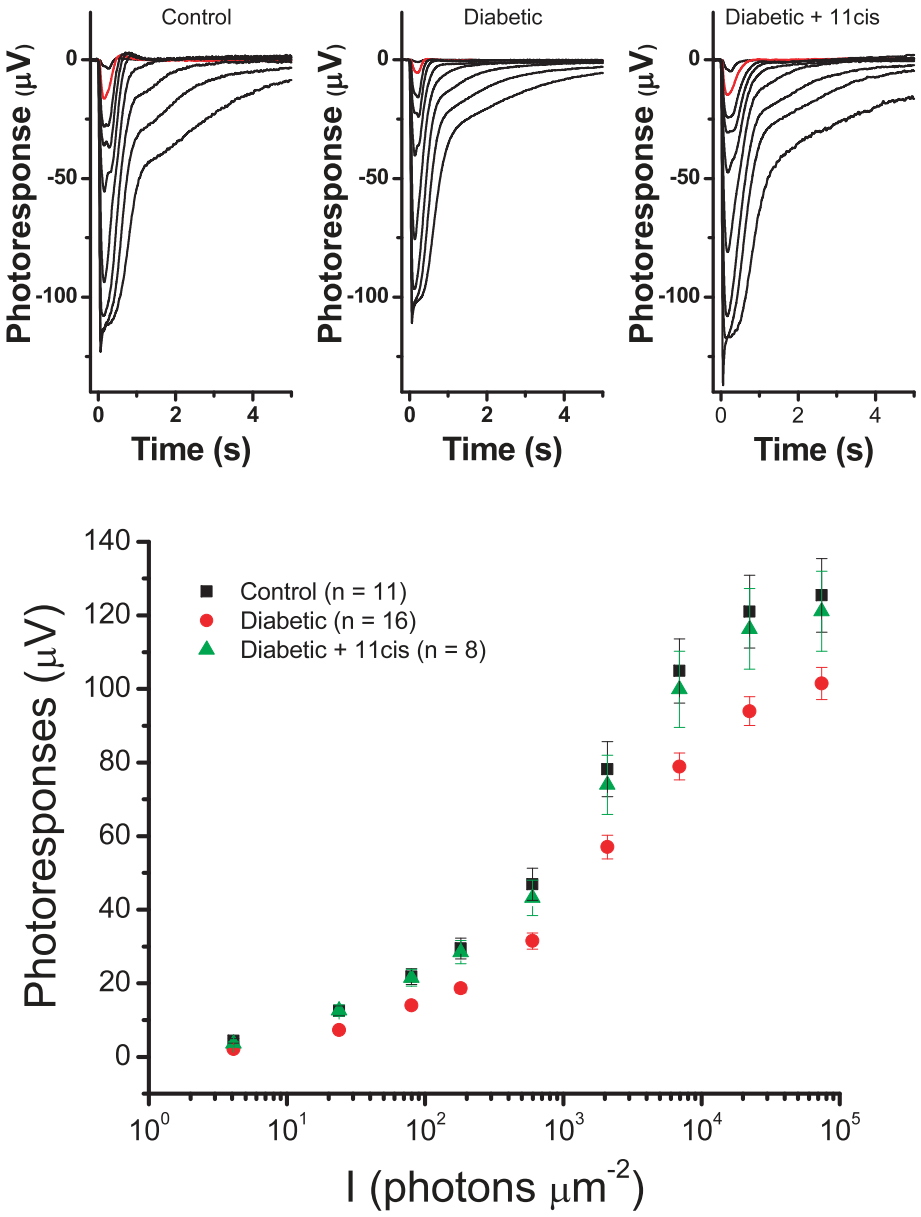

Figure 1. (*Top*) Representative rod response families from transretinal recordings of control (*left*), diabetic (*center*), and diabetic and 11-*cis*-retinaldehyde-treated (*right*) mouse retinas. Flash intensities increased in steps of 0.5 log, and *red* traces in the three panels represent responses to an identical flash intensity of 24 photons μm^{-2}. (*Bottom*) Averaged rod intensity response data from control, diabetic, and 11-*cis*-retinaldehyde-treated diabetic retinas.

considered statistically significant. Data are means ± standard error of the mean (SEM) unless otherwise noted. In all cases, a *P* value of ≤ 0.05 was considered statistically significant.

Results

Model Characteristics

Compared with age-matched controls, the body weights of the untreated diabetics were 0.61- to 0.83-fold lower across groups, and the % glycated hemoglobin concentrations of diabetes mice were 1.8- to 2.6-fold higher across groups; for the treated diabetics, body weights were 0.62- to 0.78-fold lower across groups, and the percentages of glycated hemoglobin were 1.8- to 2.65-fold greater across groups. Body weights were not collected for the control, diabetic, and diabetic + 11-*cis*-retinaldehyde mice study by OKT or by electrophysiology. Also, the % of glycated hemoglobin for the diabetic + 11-*cis*-retinaldehyde mice studied by electrophysiology was not measured; however those retinas were randomly selected from a group of diabetic mice whose untreated arm had % glycated hemoglobin that was 2.1 fold greater than controls so we feel it is reasonable to assume that the treated arm had a similar level of % glycated hemoglobin.

11-*cis*-Retinaldehyde Treatment

Transretinal Recording. Transretinal recordings revealed that the maximal rod response is reduced in diabetic retinas

Investigative Ophthalmology & Visual Science

Table. Rod Response Parameters From Transretinal Recordings

Parameter*	R_{max}, mv	$I_{1/2}$, photons mm^{-2}
Control, $n = 11$	125 ± 7	1124 ± 164
Diabetic mice, $n = 16$	102 ± 5†	1598 ± 176
Diabetic + 11-*cis*–treated mice, $n = 8$	121 ± 6‡	1159 ± 181

R_{max}, maximum response measured from bright saturating test flashes. $I_{1/2}$, half-saturation light intensity estimated from intensity response data as the test flash intensity required to produce a response with an amplitude equal to half the corresponding saturated response amplitude. $I_{1/2}$ was not significantly different across the three experimental groups.

* Values are means ± SEM.

† $P < 0.05$ compared to rods from control mice.

‡ $P < 0.05$ compared to rods from diabetic mice.

compared to controls (Fig. 1, top; Table). This reduction in voltage response was fully reversed by acute application of exogenous 11-*cis*-retinaldehyde (Fig. 1, bottom; Table).

ADC MRI. ADC values in the SRS layer in dark and light conditions from non-diabetic, diabetic, or diabetic treated with 11-*cis*-retinaldehyde were compared. Diabetic mice demonstrated a lack of light-stimulated change in ADC at 88 to 100% depth (compare Figs. 2A, 2B) (29); we do not know yet how to interpret the significant changes in ADC outside of the SRS volume. Notably, a single injection of 11-*cis*-retinaldehyde to diabetic mice largely restored the light-dependent expansion in the SRS layer to normal levels (Fig. 2C).

OKT. Behavioral tests demonstrated that diabetic mice have significantly reduced photopic SFT (Fig. 3A) and CS (Fig. 3B). A single injection of 11-*cis*-retinaldehyde corrected the CS defect (Figure 3A) but not the reduced SFT (Fig. 3B).

Superoxide Production. As expected, in freshly isolated retina, diabetes significantly increased ($P < 0.0001$) retinal content of superoxide, which is mostly generated by

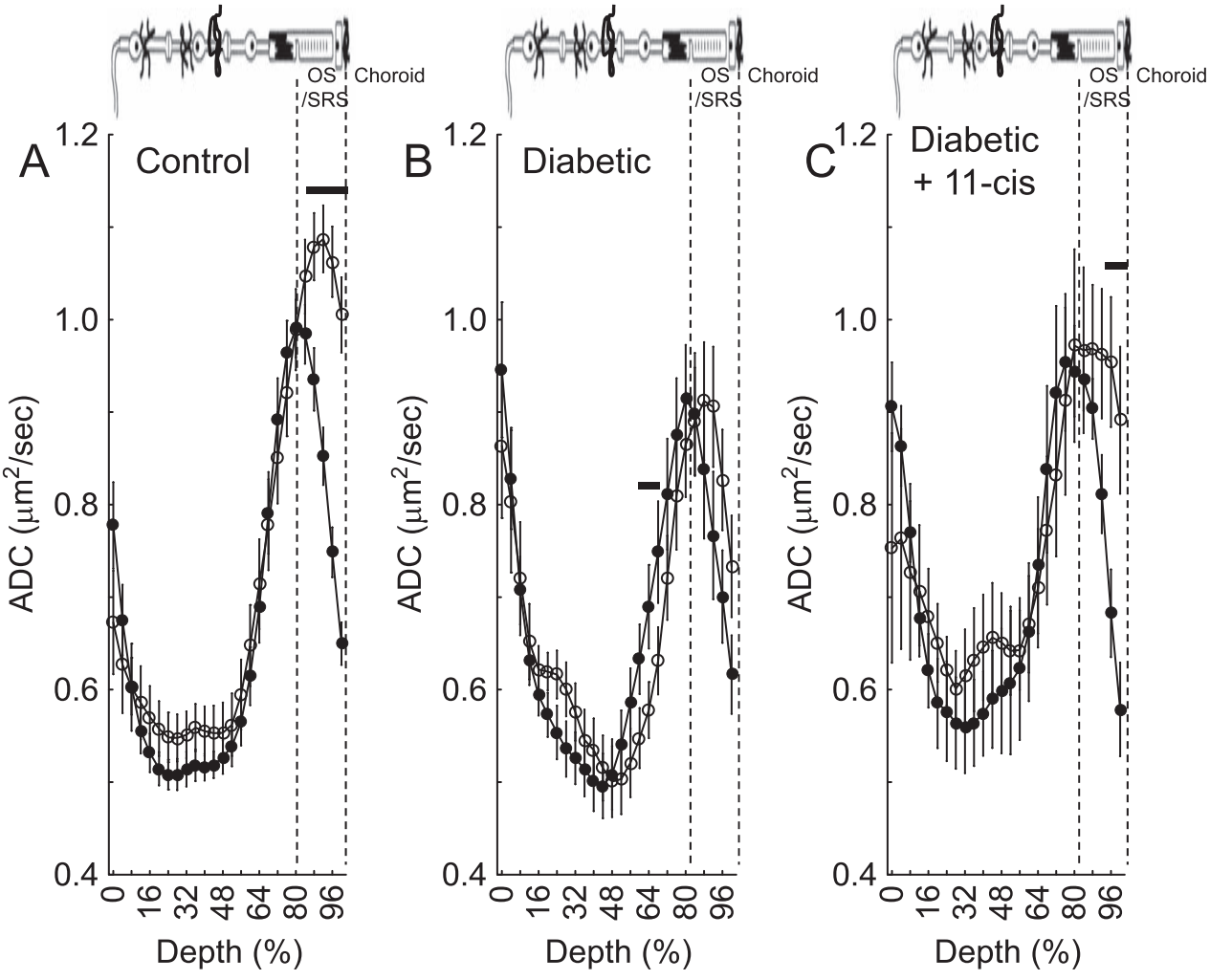

Figure 2. Summary of central retinal ADC profiles as a function of retinal depth during dark (*closed symbols*) and 20 minutes of ~500 l× light (*open symbols*) (**A**) untreated non-diabetic wild-type mice, (**B**) diabetic mice, and (**C**) 11-*cis*-retinyaldhyde-treated diabetic mice. Approximate location of outer segments (OS), subretinal spaces (SRS), and choroid are indicated by *dotted vertical lines* and the cartoon at the *top* (modified from Wangsa-Wirawan ND, Linsenmeier RA. Retinal oxygen: fundamental and clinical aspects. *Arch Ophthalmol*. 2003;121:547–557).[76] Profiles were spatially normalized to dark-adapted retinal thickness (0% = vitreous/retina border; 100% = retina/choroid border). Data are means ± SEM. *Black horizontal line* = region with significant differences ($P < 0.05$) between profiles.

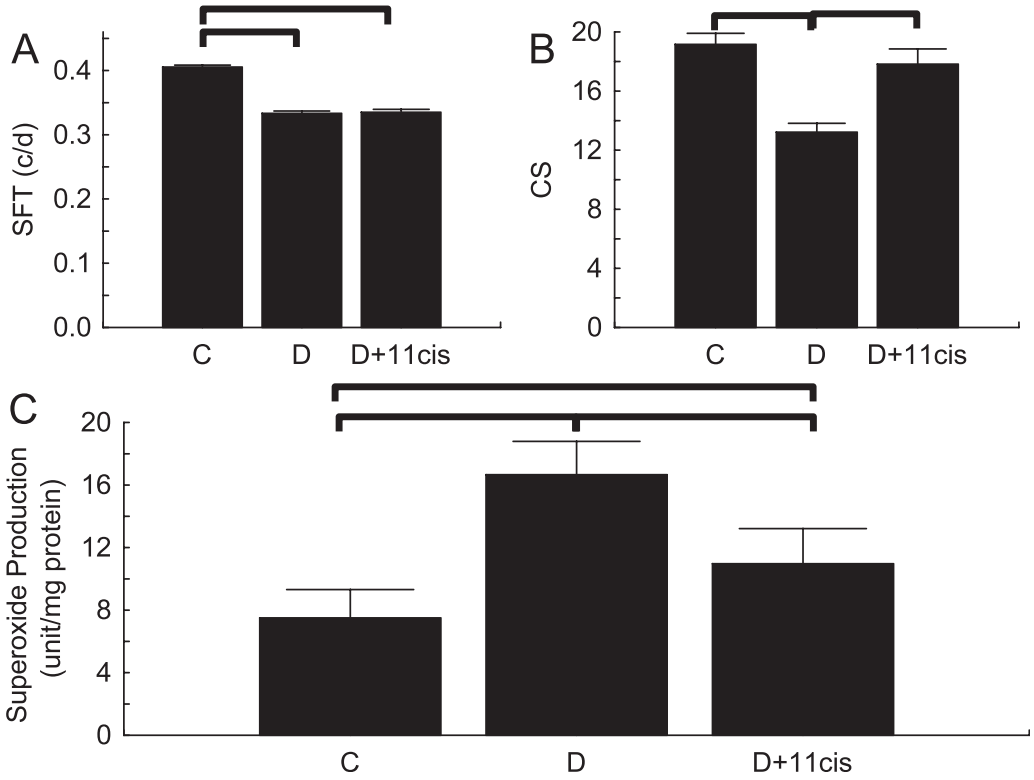

Figure 3. Summary of visual performance (**A**, **B**) and superoxide production (**C**) in untreated non-diabetic mice (C), untreated diabetic mice (D), and 11-*cis*-retinaldehyde–treated diabetic mice (D+11-*cis*). *Black line* = significant differences between bars as indicated. Data are means ± SEM (*top row*) and means ± 0.95 CI (*bottom row*).

rod cells (Fig. 3C). Diabetic mice treated with a single systemic injection of 11-*cis*-retinaldehyde had a significant reduction ($P < 0.0005$) in this oxidative stress. However, a significant difference ($P < 0.03$) in superoxide production still remained between non-diabetic and treated diabetic groups (Fig. 3C).

All-*trans*-Retinaldehyde Treatment

We also asked whether all-*trans*-retinaldehyde, the photoisomerization product of 11-*cis*-retinaldehyde in the retina,[54] might also reduce retinal superoxide production in diabetic mice. Compared with the production of superoxide in the retina of control mice (12.3 ± 1.8 units/mg protein, mean ±0.95*confidence interval), that in diabetic mice was again found to be supernormal (24.1 ± 2.6 units/mg protein, $P < 0.0001$) and was fully corrected ($P < 0.0001$) following treatment with all-*trans*-retinaldehyde (15.0 ± 3.4 units/mg protein).

9-*cis*-Retinaldehyde Treatment

OKT. 9-*cis*-Retinaldehyde treatment corrected the diabetes-induced defects in SFT (Fig. 4A) and CS (Fig. 4B). In control and diabetic mice, the presence or absence of Matrigel did not alter these findings (SFT without matrigel: 0.412 ± 0.002 c/d [$n = 5$] vs. with matrigel: 0.410 ± 0.003 c/d [$n = 8$], $P > 0.05$); contrast sensitivity (inverse Michelson contrast [unitless]) without Matrigel: 19.0 ± 0.8 ($n = 5$) versus with Matrigel (17.3 ± 0.6 [$n = 8$]; $P > 0.05$).

Superoxide Production. Diabetic mice treated with 9-*cis*-retinaldehyde also demonstrated a significant correction ($P < 0.0001$) of the diabetes-induced increase in superoxide production (Fig. 4C). However, the retinaldehyde treatment of the diabetic mice did not restore completely their level of superoxide production back to non-diabetic levels ($P < 0.003$) (Fig. 4C).

Discussion

In this study, we used transretinal recording, ADC MRI, and OKT to evaluate rod- and cone-based visual performance dysfunction in diabetic mice, and its correction with 11-*cis*- or 9-*cis*-retinaldehyde. Retinaldehyde treatments likewise inhibited retinal production of superoxide in diabetes. Because previous studies indicated that classical antioxidants improved diabetes-induced defects in retinal function, we infer that the antioxidant properties of retinaldehyde treatment were likely responsible for correction of diabetes-impaired photoreceptor dysfunction.

The most common method for evaluating rod photoreceptor function in vivo is the electroretinogram (ERG), which measures an integrated panretinal signal. While ERG can be useful to evaluate the impact of an antioxidant on diabetes-induced rod dysfunction, ERG provide no spatial resolution.[55–59] Multifocal ERG can distinguish electrical responses from different regions panretinally but suffers from extensive light scattering in small rodent eyes.[60,61] To address these problems, a new approach has been developed (and used herein) that examines responses from a small piece of retina ex vivo (i.e., transretinal recordings).[62] In addition, two other non-ERG methods have been developed that can specifically evaluate with high panretinal and transretinal (i.e., across the

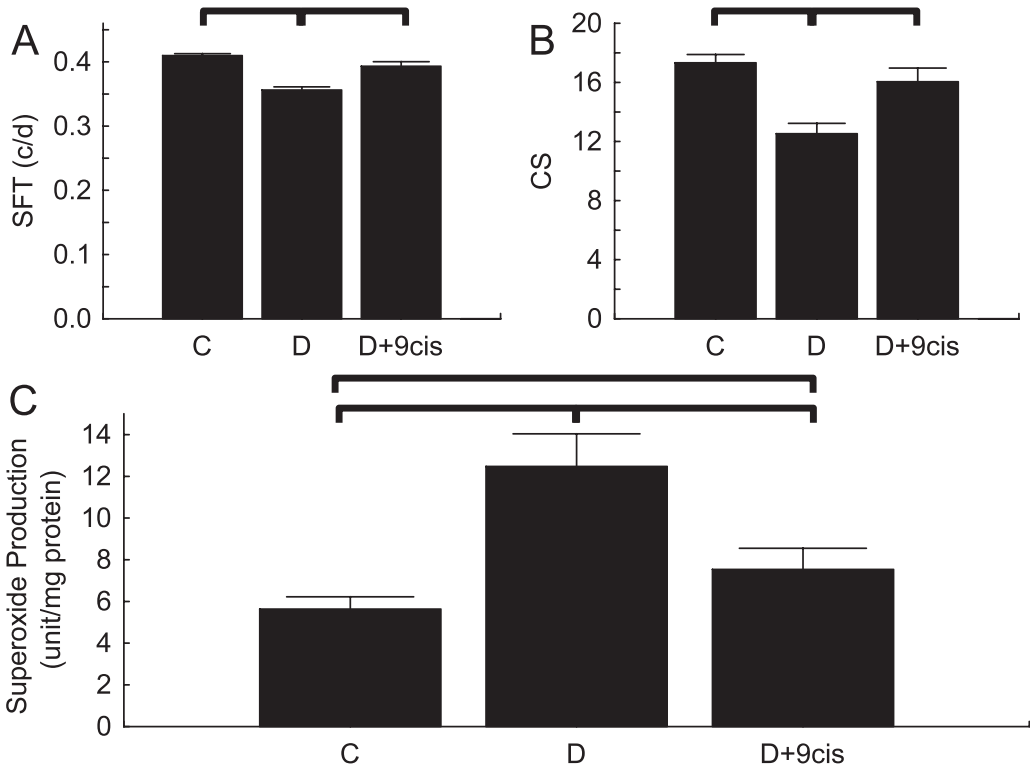

Figure 4. Summary of visual performance (*top row*) and superoxide production (*bottom row*) in untreated non-diabetic mice (**C**), untreated diabetic mice (**D**), and 9-*cis*-retinaldehyde–treated diabetic mice (D+9-*cis*). *Black line* = significant differences between bars as indicated. Data are means ± SEM (*top row*) and means ± 0.95 CI (*bottom row*).

retina) spatial resolution rod dysfunction in diabetic mice in vivo: MEMRI and ADC MRI.[3,4,29] MEMRI is the imaging modality of choice for mapping central retinal L-type calcium channel activity in rods and ADC MRI maps light-evoked subretinal space expansion, an event controlled in part by rod phototransduction and in part by retinal pigment epithelium.[29,63–68] Classical antioxidant approaches, such as administration of exogenous α-lipoic acid or overexpression of copper/zinc superoxide dismutase, also effectively correct diabetes-induced rod dysfunction as measured by MEMRI or ADC MRI.[3,4,29] Collectively, the results from transretinal recordings (Fig. 1), MEMRI,[3] and ADC MRI (Fig. 2) demonstrate that rod dysfunction in diabetes is corrected by acute 11-*cis*-retinaldehyde treatment.

Less is known about the impact of antioxidants on diabetes-induced cone dysfunction. Diabetes clearly reduces cone–based vision as measured by photopic OKT (Aung MH, et al. *IOVS* 2011;52:ARVO E-Abstract 5960).[36,37,69] Further variety of treatments correct the diabetes-dependent OKT impairment, although the impact of classical antioxidants has not been studied.[69] Here, retinaldehyde treatment was found to largely correct diabetes-suppressed cone-based vision. The beneficial OKT outcomes following retinaldehyde treatment is likely due to their antioxidant properties but more work is needed to clarify this possibility.

In an assay using ascorbic acid-induced lipid peroxidation in rat brain mitochondria, retinaldehyde (isoform not specified) was a more potent antioxidant than catalase and vitamin E, among others.[35] In other studies, vitamin A and retinoids were found to exhibit concentration-dependent anti or pro-oxidant effects.[32–35,70–73] Thus, it is not universally accepted that all retinaldehydes induce oxidative stress in all conditions. One possible explanation for these disparate findings is that retinaldehydes act in a hermetic fashion as antioxidants in low concentrations and pro-oxidants at higher levels. In any event, based on the literature it was unclear if retinaldehydes would have antioxidant properties in the present context of the retina and diabetes.[4,5,29,74] Our data present undisputable evidence that retinoids administered systemically lower the level of retinal oxidative stress and correct three assays of rod function (transretinal recordings, MEMRI, and ADC), an unlikely scenario if all-*trans* is toxic in our diabetic model.[6]

These results may seem surprising given other evidence that strong light in non-diabetic models increased levels of all-*trans*-retinaldehyde, which presumably activated NADPH oxidase, thus killing the photoreceptor.[73] However, in a separate study, we did not find that diabetes altered all-*trans*-retinaldehyde levels compared to that in age-matched non-diabetic mice.[75] Also little or no photoreceptor death has been reported in the diabetic mouse model.[6] Diabetes does, however, result in activation of retinal NADPH oxidase because apocynin can correct the diabetes-induced lesions.[1,6] Thus, diabetes causes oxidative stress independent of all-*trans*-retinaldehyde. In a separate study, we reported that another systemically administered retinoid, retinylamide, also had antioxidant activity in diabetic mice.[75] More work is needed to determine whether exogenous retinoids are acting directly or via downstream metabolites to reduce oxidative stress in the diabetic mouse. However, given the agreement in the various experimental conditions used herein, it does not appear that the mode of administration (acute versus prolonged; injection versus matrigel) or vehicle content were important variables modulating the results.

In summary, the benefits of exogenously administered retinaldehydes on electrophysiological, MRI, and OKT examinations are consistent with their antioxidant properties in the diabetic mouse.

Acknowledgments

Supported by National Institutes of Health Animal Models of Diabetic Complications Consortium and mouse metabolic phenotyping centers pilot and feasibility programs (BAB); Juvenile Diabetes Research Foundation (BAB); an unrestricted grant from Research to Prevent Blindness (Kresge Eye Institute); the Wayne State University School of Medicine MD/PhD program (DB); and NIH grants AG034752 (DB), EY00300 (TK), EY021126 and EY019312 (VJK), and EY002687 to the Department of Ophthalmology and Visual Sciences at Washington University.

Disclosure: **B.A. Berkowitz**, None; **T.S. Kern**, None; **D. Bissig**, None; **P. Patel**, None; **A. Bhatia**, None; **V.J. Kefalov**, None; **R. Roberts**, None

References

1. Du Y, Veenstra A, Palczewski K, Kern TS. Photoreceptor cells are major contributors to diabetes-induced oxidative stress and local inflammation in the retina. *Proc Natl Acad Sci U S A*. 2013;110:16586–16591.
2. Kowluru RA, Kowluru A, Mishra M, Kumar B. Oxidative stress and epigenetic modifications in the pathogenesis of diabetic retinopathy. *Prog Retin Eye Res*. 2015;pii:S1350-9462(15)00031-2.
3. Berkowitz BA, Bissig D, Patel P, Bhatia A, Roberts R. Acute systemic 11-*cis*-retinal intervention improves abnormal outer retinal ion channel closure in diabetic mice. *Mol Vis*. 2012;18:372–376.
4. Berkowitz BA, Gradianu M, Bissig D, Kern TS, Roberts R. Retinal ion regulation in a mouse model of diabetic retinopathy: natural history and the effect of Cu/Zn superoxide dismutase overexpression. *Invest Ophthalmol Vis Sci* 2009;50:2351–2358.
5. Berkowitz BA, Roberts R, Stemmler A, Luan H, Gradianu M. Impaired apparent ion demand in experimental diabetic retinopathy: correction by lipoic Acid. *Invest Ophthalmol Vis Sci*. 2007;48:4753–4758.
6. Du Y, Cramer M, Lee CA, et al. Adrenergic and serotonin receptors affect retinal superoxide generation in diabetic mice: relationship to capillary degeneration and permeability. *FASEB J*. 2015;29:2194–22204.
7. Agostinho P, Duarte CB, Carvalho AP, Oliveira CR. Oxidative stress affects the selective ion permeability of voltage-sensitive Ca2+ channels in cultured retinal cells. *Neuroscience Res*. 1997;27:323–334.
8. Shirotani K, Katsura M, Higo A, et al. Suppression of Ca2+ influx through L-type voltage-dependent calcium channels by hydroxyl radical in mouse cerebral cortical neurons. *Brain Res Mol Brain Res*. 2001;92:12–18.
9. MacGregor LC, Matschinsky FM. Altered retinal metabolism in diabetes. II. Measurement of sodium-potassium ATPase and total sodium and potassium in individual retinal layers. *J Biol Chem*. 1986;261:4052–4058.
10. Phipps JA, Yee P, Fletcher EL, Vingrys AJ. Rod photoreceptor dysfunction in diabetes: activation, deactivation, and dark adaptation. *Invest Ophthalmol Vis Sci* 2006;47:3187–3194.
11. Berkowitz BA, Gradianu M, Bissig D, Kern TS, Roberts R. Retinal ion regulation in a mouse model of diabetic retinopathy: natural history and the effect of Cu/Zn superoxide dismutase overexpression. *Invest Ophthalmol Vis Sci*. 2009;50:2351–2358.
12. Ramos de Carvalho JE, Verbraak FD, Aalders MC, van Noorden CJ, Schlingemann RO. Recent advances in ophthalmic molecular imaging. *Surv Ophthalmol*. 2014;59:393–413.
13. Berkowitz BA, Bissig D, Dutczak O, Corbett S, North R, Roberts R. MRI biomarkers for evaluation of treatment efficacy in preclinical diabetic retinopathy. *Expert Opin Med Diagn*. 2013;7:393–403.
14. Berkowitz BA, Roberts R, Oleske DA, et al. Quantitative mapping of ion channel regulation by visual cycle activity in rodent photoreceptors in vivo. *Invest Ophthalmol Vis Sci* 2009;50:1880–1885.
15. Berkowitz BA, Gradianu M, Schafer S, et al. Ionic dysregulatory phenotyping of pathologic retinal thinning with manganese-enhanced MRI. *Invest Ophthalmol Vis Sci* 2008;49:3178–3184.
16. Berkowitz BA, Roberts R, Goebel DJ, Luan H. Noninvasive and simultaneous imaging of layer-specific retinal functional adaptation by manganese-enhanced MRI. *Invest Ophthalmol Vis Sci*. 2006;47:2668–2674.
17. Drapeau P, Nachshen DA. Manganese fluxes and manganese-dependent neurotransmitter release in presynaptic nerve endings isolated from rat brain. *J Physiol*. 1984;348:493–510.
18. Carlson RO, Masco D, Brooker G, Spiegel S. Endogenous ganglioside GM1 modulates L-type calcium channel activity in N18 neuroblastoma cells. *J Neurosci* 1994;14:2272–2281.
19. Cross DJ, Flexman JA, Anzai Y, et al. In vivo manganese MR imaging of calcium influx in spontaneous rat pituitary adenoma. *AJNR Am J Neuroradiol*. 2007;28:1865–1871.
20. Berkowitz BA, Bissig D, Bergman D, Bercea E, Kasturi VK, Roberts R. Intraretinal calcium channels and retinal morbidity in experimental retinopathy of prematurity. *Mol Vis*. 2011;17:2516–2526.
21. Berkowitz BA, Roberts R, Penn JS, Gradianu M. High-resolution manganese-enhanced MRI of experimental retinopathy of prematurity. *Invest Ophthalmol Vis Sci* 2007;48:4733–4740.
22. Tofts PS, Porchia A, Jin Y, Roberts R, Berkowitz BA. Toward clinical application of manganese-enhanced MRI of retinal function. *Brain Res Bull*. 2010;81:333–338.
23. Berkowitz BA, Roberts R, Oleske DA, et al. Quantitative mapping of ion channel regulation by visual cycle activity in rodent photoreceptors in vivo. *Invest Ophthalmol Vis Sci* 2009;50:1880–1885.
24. Ostroy SE. Altered rhodopsin regeneration in diabetic mice caused by acid conditions within the rod photoreceptors. *Curr Eye Res*. 1998;17:979–985.
25. Ostroy SE, Frede SM, Wagner EF, Gaitatzes CG, Janle EM. Decreased rhodopsin regeneration in diabetic mouse eyes. *Invest Ophthalmol Vis Sci* 1994;35:3905–3909.
26. Garcia-Ramírez M, Hernández C, Villarroel M, et al. Interphotoreceptor retinoid-binding protein (IRBP) is downregulated at early stages of diabetic retinopathy. *Diabetologia*. 2009;52:2633–2641.
27. Kirwin SJ, Kanaly ST, Hansen CR, Cairns BJ, Ren M, Edelman JL. Retinal gene expression and visually evoked behavior in diabetic long Evans rats. *Invest Ophthalmol Vis Sci*. 2011;52:7654–7663.
28. Berkowitz BA, Gorgis J, Patel A, et al. Development of an MRI biomarker sensitive to tetrameric visual arrestin 1 and its reduction via light-evoked translocation in vivo. *FASEB J*. 2015;29:554–564.
29. Berkowitz BA, Grady EM, Khetarpal N, Patel A, Roberts R. Oxidative stress and light-evoked responses of the posterior segment in a mouse model of diabetic retinopathy. *Invest Ophthalmol Vis Sci*. 2015;56:606–615.
30. Ottlecz A, Bensaoula T. Captopril ameliorates the decreased Na+,K(+)-ATPase activity in the retina of streptozotocin-induced diabetic rats. *Invest Ophthalmol Vis Sci* 1996;37:1633–1641.

31. Doly M, Droy-Lefaix MTrs, Braquet P. Oxidative stress in diabetic retina. In: Emerit I, Chance B, eds. *Free Radicals and Aging.* 62nd ed. Basel: Birkháuser; 1992;299–307.
32. Keys SA, Zimmerman WF. Antioxidant activity of retinol, glutathione, and taurine in bovine photoreceptor cell membranes. *Exp Eye Res*. 1999;68:693–702.
33. Zanotto-Filho A, Schröder R, Moreira JC. Xanthine oxidase-dependent ROS production mediates vitamin A pro-oxidant effects in cultured Sertoli cells. *Free Radic Res*. 2008;42:593–601.
34. Mantymaa P, Guttorm T, Siitonen T, et al. Cellular redox state and its relationship to the inhibition of clonal cell growth and the induction of apoptosis during all-*trans* retinoic acid exposure in acute myeloblastic leukemia cells. *Haematologica*. 2000;85:238–245.
35. Das NP. Effects of vitamin A and its analogs on nonenzymatic lipid peroxidation in rat brain mitochondria. *J Neurochem*. 1989;52:585–588.
36. Cahill H, Nathans J. The optokinetic reflex as a tool for quantitative analyses of nervous system function in mice: application to genetic and drug-induced variation. *PLoS One*. 2008;3:e2055.
37. Akimov NP, Rentería RC. Spatial frequency threshold and contrast sensitivity of an optomotor behavior are impaired in the Ins2Akita mouse model of diabetes. *Behav Brain Res*. 2012;226:601–605.
38. Muir ER, Rentería RC, Duong TQ. Reduced ocular blood flow as an early indicator of diabetic retinopathy in a mouse model of diabetes. *Invest Ophthalmol Vis Sci*. 2012;53:6488–6494.
39. Umino Y, Solessio E. Loss of scotopic contrast sensitivity in the optomotor response of diabetic mice. *Invest Ophthalmol Vis Sci*. 2013;54:1536–1543.
40. Lee CA, Li G, Patel MD, et al. Diabetes-induced impairment in visual function in mice: contributions of p38 MAPK, RAGE, leukocytes, and aldose reductase. *Invest Ophthalmol Vis Sci*. 2014;55:2904–2910.
41. Tang PH, Fan J, Goletz PW, Wheless L, Crouch RK. Effective and sustained delivery of hydrophobic retinoids to photoreceptors. *Invest Ophthalmol Vis Sci*. 2010;51:5958–5964.
42. Douglas RM, Alam NM, Silver BD, McGill TJ, Tschetter WW, Prusky GT. Independent visual threshold measurements in the two eyes of freely moving rats and mice using a virtual-reality optokinetic system. *Vis.Neuro*. 2005;22:677–684.
43. Du Y, Miller CM, Kern TS. Hyperglycemia increases mitochondrial superoxide in retina and retinal cells. *Free Radic Biol Med*. 2003;35:1491–1499.
44. Kern TS, Miller CM, Du Y, et al. Topical administration of nepafenac inhibits diabetes-induced retinal microvascular disease and underlying abnormalities of retinal metabolism and physiology. *Diabetes*. 2007;56:373–379.
45. Gubitosi-Klug RA, Talahalli R, Du Y, Nadler JL, Kern TS. 5-Lipoxygenase, but not 12/15-lipoxygenase, contributes to degeneration of retinal capillaries in a mouse model of diabetic retinopathy. *Diabetes*. 2008;57:1387–1393.
46. Du Y, Tang J, Li G, et al. Effects of p38 MAPK inhibition on early stages of diabetic retinopathy and sensory nerve function. *Invest Ophthalmol Vis Sci*. 2010;51:2158–2164.
47. Kern TS, Du Y, Miller CM, Hatala DA, Levin LA. Overexpression of Bcl-2 in vascular endothelium inhibits the microvascular lesions of diabetic retinopathy. *Am J Pathol*. 2010;176:2550–2558.
48. Sillman AJ, Ito H, Tomita T. Studies on the mass receptor potential of the isolated frog retina. I. General properties of the response. *Vision Res*. 1969;9:1435–1442.
49. Vinberg F, Kolesnikov AV, Kefalov VJ. Ex vivo ERG analysis of photoreceptors using an in vivo ERG system. *Vision Res*. 2014;101:108–117.
50. Bissig D, Berkowitz BA. Light-dependent changes in outer retinal water diffusion in rats in vivo. *Mol Vis*. 2012;18:2561–2577.
51. Berkowitz BA, Grady EM, Roberts R. Confirming a prediction of the calcium hypothesis of photoreceptor aging in mice. *Neurobiol Aging*. 2014;35:1883–1891.
52. Bissig D, Berkowitz BA. Same-session functional assessment of rat retina and brain with manganese-enhanced MRI. *Neuroimage*. 2011;58:749–760.
53. Liang Z. Longitudinal data analysis using generalized linear models. *Biometrika*. 1986;73:13–22.
54. Lamb TD, Pugh J. Dark adaptation and the retinoid cycle of vision. *Prog Retin Eye Res*. 2004;23:307–380.
55. Barile GR, Pachydaki SI, Tari SR, et al. The RAGE axis in early diabetic retinopathy. *Invest Ophthalmol Vis Sci*. 2005;46:2916–2924.
56. Midena E, Segato T, Radin S, et al. Studies on the retina of the diabetic db/db mouse. I. Endothelial cell-pericyte ratio. *Ophthalmic Res*. 1989;21:106–111.
57. Horio N, Clermont AC, Abiko A, et al. Angiotensin AT(1) receptor antagonism normalizes retinal blood flow and acetylcholine-induced vasodilatation in normotensive diabetic rats. *Diabetologia*. 2004;47:113–123.
58. Johnsen-Soriano S, Garcia-Pous M, Arnal E, et al. Early lipoic acid intake protects retina of diabetic mice. *Free Radic Res*. 2008;42:613–617.
59. Samuels IS, Lee CA, Petrash JM, Peachey NS, Kern TS. Exclusion of aldose reductase as a mediator of ERG deficits in a mouse model of diabetic eye disease. *Vis Neurosci*. 2012;29:267–274.
60. Ball SL, Petry HM. Noninvasive assessment of retinal function in rats using multifocal electroretinography. *Invest Ophthalmol Vis Sci*. 2000;41:610–617.
61. Nusinowitz S, Ridder WH, Heckenlively JR. Rod multifocal electroretinograms in mice. *Invest Ophthalmol Vis Sci*. 1999;40:2848–2858.
62. Kolesnikov AV, Kefalov VJ, Transretinal ERG. Recordings from mouse retina: rod and cone photoresponses. *J Vis Exp*. 2012;3424.
63. Adijanto J, Banzon T, Jalickee S, Wang NS, Miller SS. CO2-induced ion and fluid transport in human retinal pigment epithelium. *J Gen Physiol*. 2009;133:603–622.
64. Cao W, Govardovskii V, Li JD, Steinberg RH. Systemic hypoxia dehydrates the space surrounding photoreceptors in the cat retina. *Invest Ophthalmol Vis Sci*. 1996;37:586–596.
65. Li JD, Govardovskii VI, Steinberg RH. Light-dependent hydration of the space surrounding photoreceptors in the cat retina. *Vis Neurosci*. 1994;11:743–752.
66. Gallemore RP, Li JD, Govardovskii VI, Steinberg RH. Calcium gradients and light-evoked calcium changes outside rods in the intact cat retina. *Vis Neurosci*. 1994;11:753–761.
67. Govardovskii VI, Li JD, Dmitriev AV, Steinberg RH. Mathematical model of TMA+ diffusion and prediction of light-dependent subretinal hydration in chick retina. *Invest Ophthalmol Vis Sci*. 1994;35:2712–2724.
68. Li JD, Gallemore RP, Dmitriev A, Steinberg RH. Light-dependent hydration of the space surrounding photoreceptors in chick retina. *Invest Ophthalmol Vis Sci*. 1994;35:2700–2711.
69. Lee CA, Li G, Patel MD, et al. Diabetes-induced impairment in visual function in mice: contributions of p38 MAPK, RAGE, leukocytes, and aldose reductase. *Invest Ophthalmol.Vis Sci*. 2014;55:2904–2910.
70. Chen Y, Okano K, Maeda T, et al. Mechanism of all-*trans*-retinal toxicity with implications for Stargardt disease and age-related macular degeneration. *J Biol.Chem*. 2012;287:5059–5069.

Investigative Ophthalmology & Visual Science

71. Li J, Cai X, Xia Q, et al. Involvement of endoplasmic reticulum stress in all-*trans*-retinal-induced retinal pigment epithelium degeneration. *Toxicol Sci*. 2015;143:196–208.
72. Lochner JE, Badwey JA, Horn W, Karnovsky ML. All-*trans*-retinal stimulates superoxide release and phospholipase C activity in neutrophils without significantly blocking protein kinase C. *Proc Natl Acad Sci U S A*. 1986;83:7673–7677.
73. Sawada O, Perusek L, Kohno H, et al. All-*trans*-retinal induces Bax activation via DNA damage to mediate retinal cell apoptosis. *Exp Eye Res*. 2014;123:27–36.
74. Masutomi K, Chen C, Nakatani K, Koutalos Y. All-*trans* retinal mediates light-induced oxidation in single living rod photoreceptors. *Photochem Photobiol*. 2012;88:1356–1361.
75. Liu H, Tang J, Du Y, et al. Retinylamine benefits early diabetic retinopathy in mice. *J Biol Chem*. 2015;290:21568–21579.
76. Wangsa-Wirawan ND, Linsenmeier RA. Retinal oxygen: fundamental and clinical aspects. *Arch Ophthalmol*. 2003;121:547–557.

Investigative Ophthalmology & Visual Science